Crystal structures of proline-derived enamines

Dominique Anna Bock, Christian W. Lehmann, and Benjamin List[1]

Max-Planck-Institut für Kohlenforschung, Kaiser-Wilhelm-Platz 1, 45470 Muelheim an der Ruhr, Germany

Edited by Eric N. Jacobsen, Harvard University, Cambridge, MA, and approved September 17, 2010 (received for review May 19, 2010)

The isolation and structural characterization of both aldehyde- and ketone-derived proline enaminones are reported and discussed. Crystal structures of 10 proline enamines provide information on stereochemical aspects, i.e., double bond configuration and *syn*- vs. *anti*-positioning of the carboxylate relative to the enamine double bond. Furthermore, the obtained crystal structures are compared with the density functional theory-calculated structures of the ground and transition state and the postulated Seebach–Eschenmoser transition state.

enamine catalysis | mechanism | organocatalysis

Within the last 10 y, *enamine catalysis*, the catalytic activation of carbonyl compounds via enamine intermediates, has grown into a powerful approach to organic synthesis (1–4). Among the many different primary and secondary amine catalysts that have been developed in this field, the amino acid proline remains a privileged motif and there are literally dozens of reaction types that are catalyzed with this wonderful natural product (5). Proline-derived enamines of aldehydes and ketones are key intermediates in the catalytic cycles of these reactions (Scheme 1) (6–13). Surprisingly though, such enamines have remained entirely hypothetical and resisted attempts at their structural characterization. Such information, however, appears to be highly valuable toward understanding the mechanistic details with which proline catalyzes carbonyl transformations. Here we report and discuss crystal structures of a series of stabilized enamines of proline and of some of its analogues.

The main difficulty in previous attempts at characterizing proline enamines has been the tendency of carbonyl compounds to reversibly react with proline giving oxazolidinones instead of the enamines (Eq. **1**). Rather than the enamine, thermodynamics favor the oxazolidinone constitutional isomer, in which one C–O- and one C–H-σ-bond are gained at the expense of one C–C-π-bond and one O–H-σ-bond:

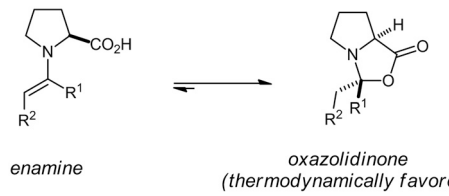

[1]

In view of the catalytic action of proline, oxazolidinone formations with aldehyde or ketone substrates are best described as *parasitic equilibria* because they are not leading to product but inhibit its formation (14). Although aldehyde-derived "Seebach oxazolidinones" (15–17) have long been known, their ketone analogues have only recently been detected and characterized by us (14) and later isolated also by Seebach et al. (18). Interestingly, the condensation product of acetone and proline has also been detected by Marquez and Metzger using mass spectrometry (19). In light of our previous careful NMR-spectroscopic characterization of this adduct as an oxazolidinone (14), their assignment as an enamine appears to be questionable. In addition, Seebach et al. have partially characterized an ammonium salt of the prolyl enamine of cyclohexanone (18). Disappointingly though, crystallographic data on proline enamines are entirely lacking. In fact, to the best of our knowledge and based on a search of the Cambridge Structural Database (CSD, Version 5.31, Nov. 2009) crystal structures of any proline-derived enamines have not been reported previously.

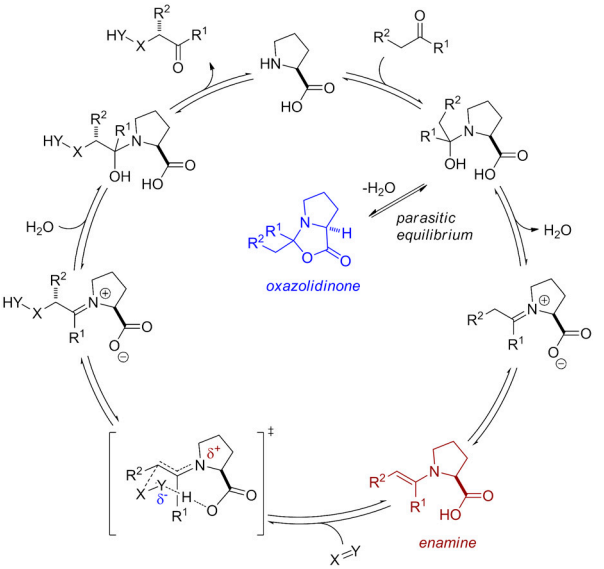

Scheme 1. General catalytic cycle of proline-catalyzed addition reactions of carbonyl compounds to electrophiles $X = Y$.

At the outset of this work several years ago, we wondered whether it is possible to crystallize proline enamines that are formally derived of 1,3-dicarbonyl compounds. We hypothesized that, in contrast to the situation of the parent unconjugated system (Eq. **1**), such structures may, in fact, be more stable than the corresponding oxazolidinones because cyclization would interrupt conjugation of the vinylogous amide system (Eq. **2**).

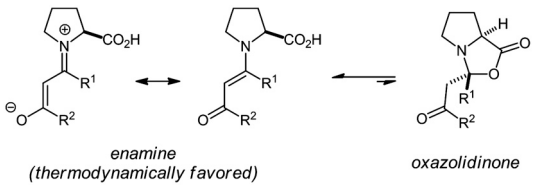

[2]

Indeed, proline-derived vinylogous amides (or enaminones) have been reported previously and characterized spectroscopically as enamines (20–23). More important for the present discus-

Author contributions: B.L. designed research; D.A.B. performed research; D.A.B., C.W.L., and B.L. analyzed data; and D.A.B., C.W.L., and B.L. wrote the paper.

The authors declare no conflict of interest.

This article is a PNAS Direct Submission.

[1]To whom correspondence should be addressed. E-mail: list@mpi-muelheim.mpg.de.

This article contains supporting information online at www.pnas.org/lookup/suppl/doi:10.1073/pnas.1006509107/-/DCSupplemental.

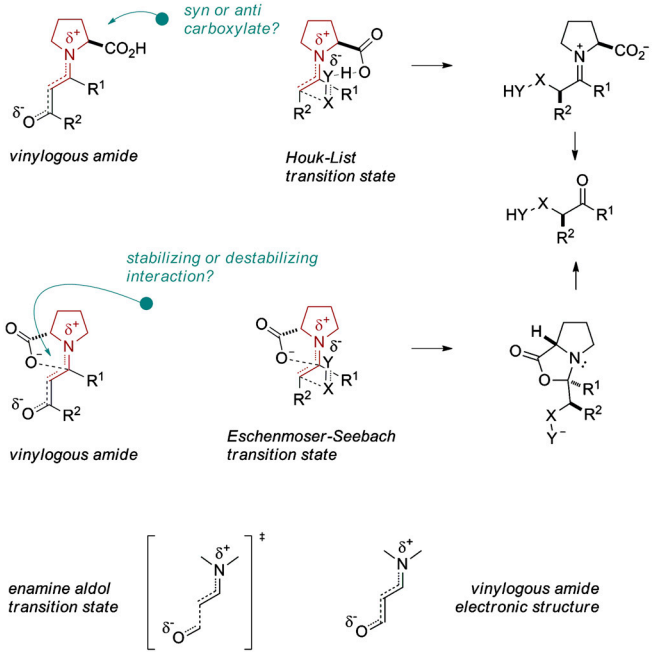

Fig. 1. Potential relationships of proline-derived vinylogous amides and the proline enamine in the transition state.

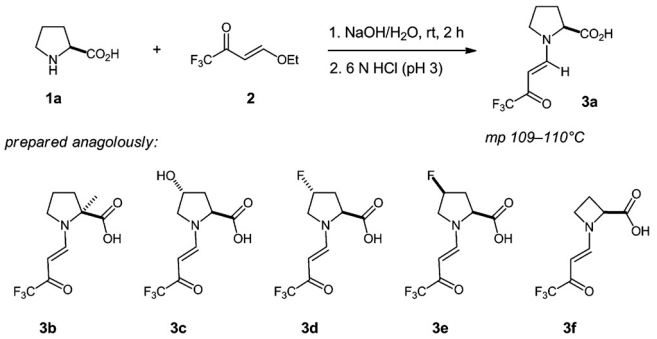

Fig. 2. Synthesis of crystalline enamine derivatives **3a–3f**.

sion is that such vinylogous amides may be considered transition state models of a proline enamine engaging in the reaction with an electrophile (Fig. 1). In both cases is electron density removed from the electron rich enamine-π-system. This electronic redistribution should impact the enamine geometry. For example, because of the partial iminium ion character of the vinylogous amide (and in fact of the corresponding bond-forming transition state), the sp^3 character and consequently pyramidalization at nitrogen should be reduced. Similarly, the enaminone conjugation will influence the bond lengths of the system such that the enamine double bond will be *longer* than that expected for the analogous unconjugated proline enamine. The C—N bond of the enamine system in turn is expected to be *shorter*, reflecting the beginning π-character of this bond. We reasoned that crystal-structural information on such vinylogous amides would provide additional valuable information on stereochemical aspects of such enamines, i.e., double bond configuration and *syn*- vs. *anti*-positioning of the carboxylate relative to the enamine double bond, which corresponds to an (*E*)- vs. (*Z*)-configuration at the forming iminium ion.

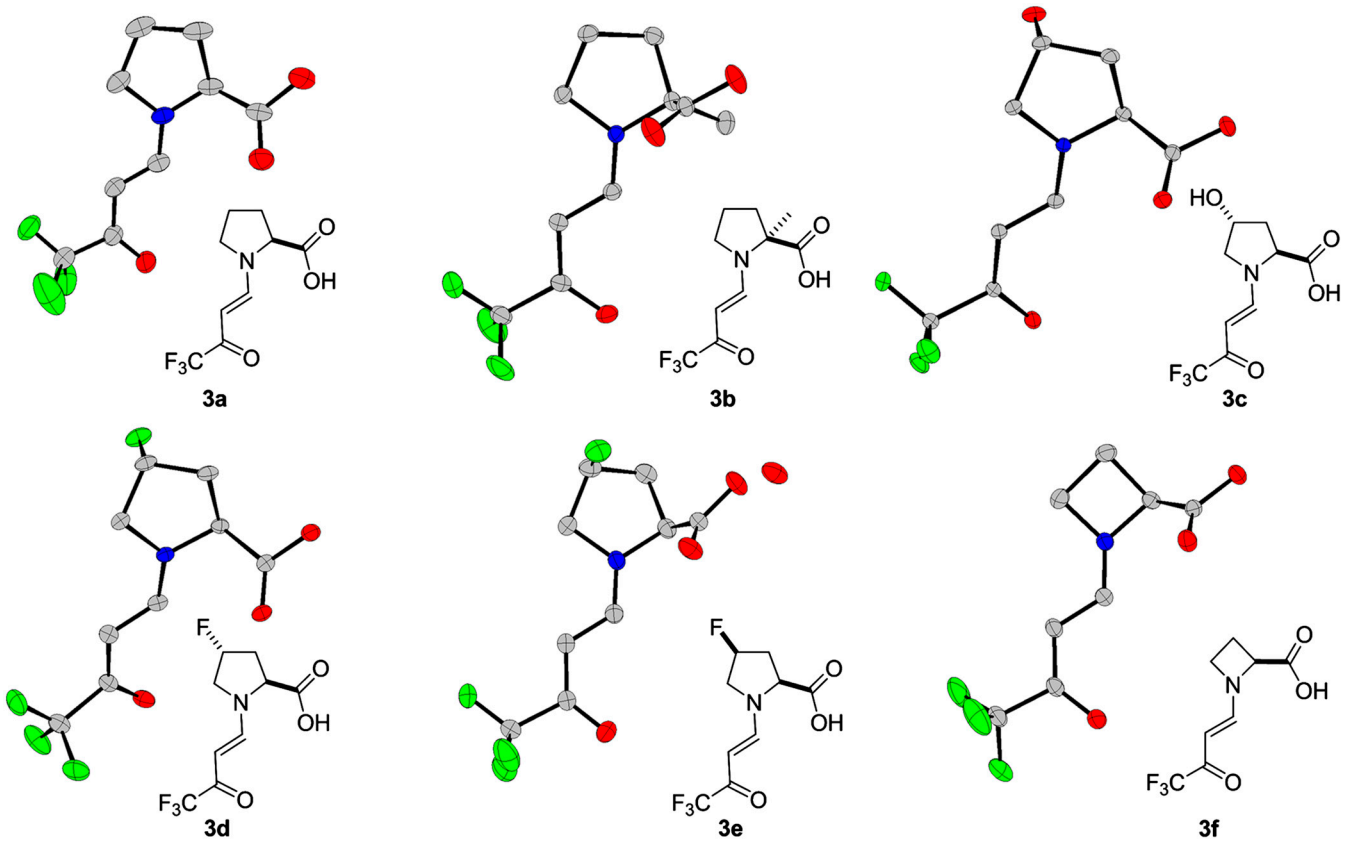

Fig 3. Crystal structures of enamines **3a–3f**.

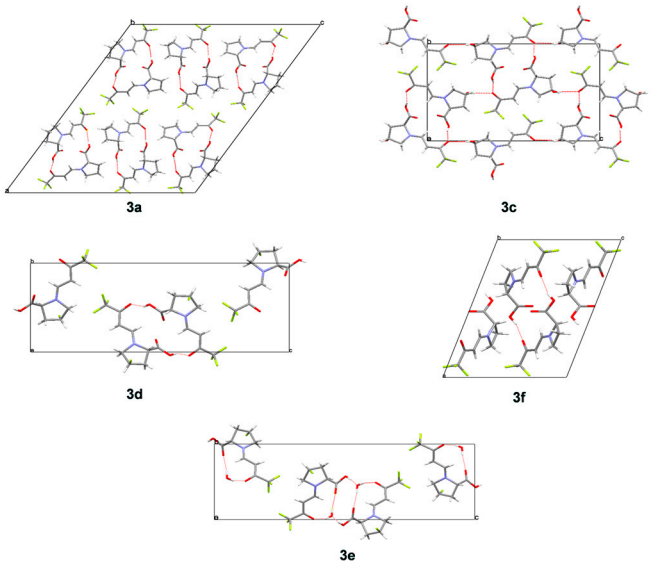

Fig. 4. Crystal packing of enamine **3a**, **3c**, **3d**, **3e**, and **3f**.

Additionally, such structural investigations may reveal the degree of oxazolidinone character in proline enaminones. According to a recent proposal by Seebach et al., the reaction of the proline enamine with an electrophile involves an anionic cyclization of the *syn*-configured carboxylate into the enamine α-carbon with concomitant bond formation at its β-carbon in the sense of an electrophile-induced lactonization (18). This mechanism has already been discussed by Hajos and Parrish before (24) and leads directly to an oxazolidinone. If the postulated bond formation between the carboxylate oxygen and the enamine α-carbon in the transition state would indeed contribute to its stabilization, the question may then be asked if such an interaction could not also occur in the corresponding vinylogous amide system. Alternatively, C—O bond formation may actually *destabilize* the enaminone by interrupting conjugation.

In any case, we were curious about the structures of proline-derived vinylogous enamines and speculated that their elucidation may potentially stimulate further thoughts on proline catalysis.

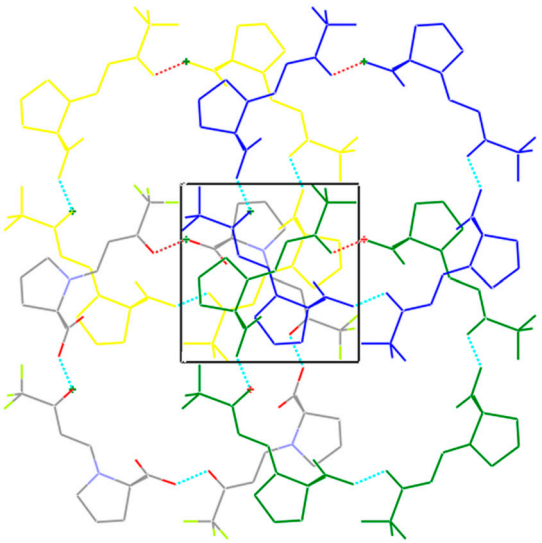

Fig. 5. Crystal packing of enamine **3b** viewed along the [001] direction. Only one strand of the helices is shown; the central pores are filled by consecutive strands.

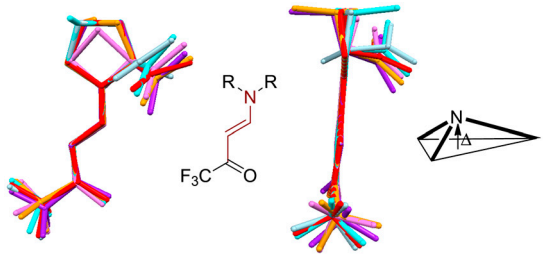

Fig. 6. Superimposition of the enamine structures **3a–3f**. The red colored atoms are superimposed. Pyramidalization Δ.

Results

As mentioned before, vinylogous amides of proline have already been reported. For example, enamine **3a** has been investigated by NMR spectroscopy and was shown to consist of a mixture of *anti* and *syn* conformers (20). We found that suitable crystals for crystal structure determination could be obtained upon treatment of (*s*)-proline with 4-ethoxy-1,1,1-trifluoro-3-buten-1-one in aqueous sodium hydroxide and crystallization from diethyl ether (25). This procedure turned out to be general, and a variety of proline derivates and analogues underwent the same reaction and furnished suitable crystals for crystal structure determination (Fig. 2).

The crystal structures of the whole series of enamines **3a–3f** could be elucidated successfully and yielded the solid-state molecular conformations shown in Fig. 3. The observed conformational trends warrant further discussion. The molecular shape of enamines **3a–3f** is determined primarily by (*i*) the C—C-double bond configuration (*E* vs. *Z*), (*ii*) the conformation of the enamine being either *syn* or *anti* to the carboxy group, and (*iii*) by the conformation of the keto group being either *s-cis* or *s-trans* to the double bond.

First it is noted that as expected, all enamines adopt an (*E*)-configuration in the solid state. Furthermore, although there is an equilibrium in solution between the *syn* and *anti* conformers in enamine **3a**, as mentioned above, enamines **3a–3f** adopt exclusively the *anti* conformation in the solid state. At the same time, all structures of this series are found to exhibit an *s-cis* conformation. This conformational preference is accompanied by the formation of hydrogen bonds leading to supramolecular aggregates. Besides the formation of dimers (**3a** and **3f**), helices and catemers are observed (Fig. 4). In all crystal structures of this series, an O—H···O=C hydrogen bond between the carboxy group as hydrogen bond donor and the (CF_3)—C=O group as hydrogen bond acceptor is present. It forms the basis of the dimer between two crystallographically independent molecules in enamine **3a** as well as in the centrosymmetric (inversion symmetry) dimer observed for enamine **3f**. The asymmetric unit of enamine **3a** contains a third independent molecule, which links via the same type of hydrogen bond in a head-to-tail fashion to the next enamine molecule, symmetry related by a 2_1-screw axis. This hydrogen-bonding motif is also present in the crystal structures of **3c**, **3d**, and **3e** (Fig. 4). In case of the monohydrate **3e**, an

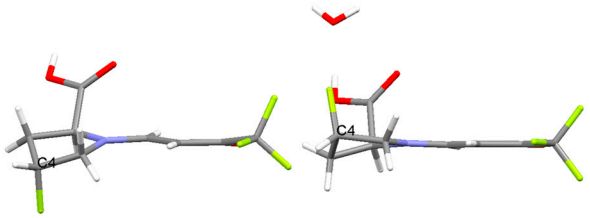

Fig. 7. Conformation of the five-membered ring at the example of **3d** and **3e** (*Left*, exo; *Right*, endo).

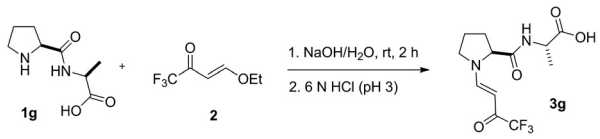

Fig. 8. Typical procedure for the synthesis of proline enamine **3g**.

additional water molecule is inserted between the carboxy donor and the carbonyl acceptor providing an additional hydrogen bond between one of the water protons and the C=O oxygen atom of the carboxy group. Remarkably this latter potential hydrogen bridge acceptor is not utilized in any of the other structures. Another stabilizing hydrogen bond is present in the structure of **3c**. It is formed between the hydroxyl substituent of the pyrrolidine ring and the trifluoromethylcarbonyl group.

In the structure of α-methyl proline derivative **3b**, hydrogen bonds between the carboxy group and the (CF_3)–C=O group are present as well. However, in this case helices are formed, utilizing the crystallographic 4_3 screw axis. The helices are entwined further (Fig. 5) via a second 4_3 symmetry operation.

In none of the structures discussed so far is the N atom significantly pyramidalized. Furthermore, the carbon–carbon double bond and the carbonyl group together with the nitrogen atom all lie in approximately the same plane. The observed bond lengths in the enamine moiety show only small and unsystematic variations. The C=C-bond distances range from 1.3817(7) Å to about 1.3964(10) Å, whereas the enamine N–C-bond distances range from 1.3034(9) Å to about 1.3144(9) Å.

Superpositioning of the enamine part of the molecular structures **3a–3f** reveals the expected flexible conformation of the CF_3 group. Small conformational variations of the five membered rings are amplified in the corresponding carboxylates (Fig. 6).

The pyrrolidines adopt a slightly twisted envelope conformation. The magnitude of the torsion angle of one of the endocyclic C–N bonds is between 4.04° and 8.5°, which forces either C3 or C4 out of the plane. In the case of **3c** and **3d** with the substituent at C4 being *trans* to the carboxy group, the flap is formed by C4 and it is pointing to the opposite side (exo) of the ring plane with respect to the carboxy group. This holds as well for one of the independent molecules of **3a**, whereas for the second molecule of **3a** the flap is formed by C3, which is pointing to the same side (endo) as the carboxy group. The flap of the envelope is also formed by C3 for enamines **3b** and **3e**; however, in these cases the flap points again to the opposite side of the plane (Fig. 7).

Suitable crystals for crystal structure determination were also obtained upon treatment of an N-prolyl peptide [(*s*)-proline-(*s*)-alanine] with 4-ethoxy-1,1,1-trifluoro-3-buten-1-one in sodium hydroxide and crystallization of the obtained enamine (**3g**) from diethyl ether (Fig. 8).

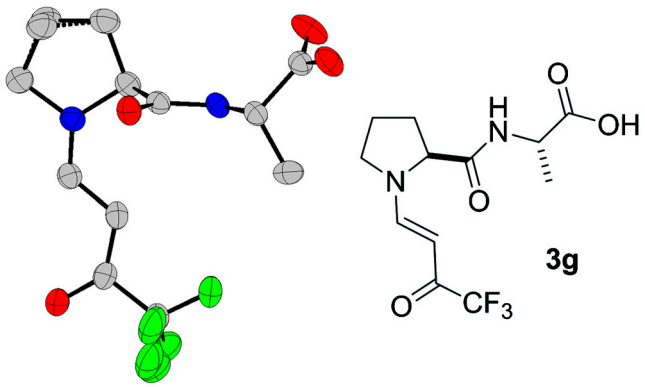

Fig. 9. Crystal structure of peptide-derived enamine **3g**.

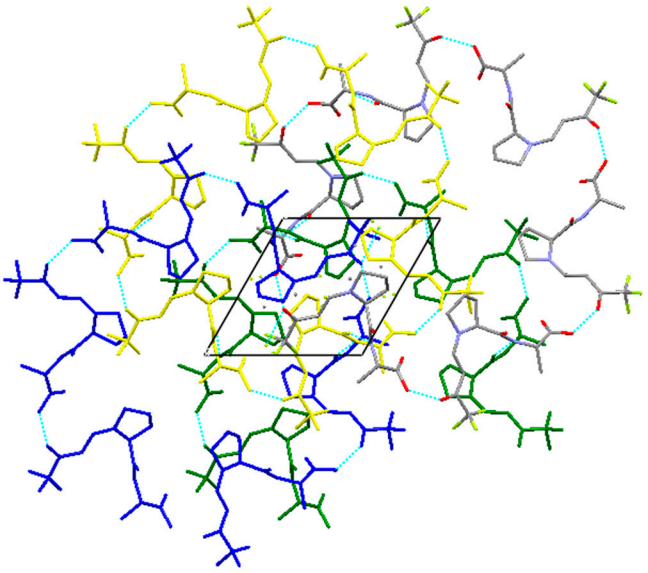

Fig. 10. Crystal structure of enamine **3g** viewed along the [010] axis.

Interestingly, and in contrast to the previously discussed crystal structures, enamine **3g** exists only in the *syn* conformation in the solid state (Fig. 9).

The enamine N–C-bond distance is 1.309(3) Å and the C=C-bond distance is 1.386(3) Å. These bond lengths are in agreement with those observed in the crystal structures of enamines **3a–3f**. Similarly, N pyramidalization (N pyramidality Δ: 0.020 Å) and planarity of the conjugated π-electron system are very similar in enamines **3a–3f**. The intermolecular interactions of this crystal structure are dominated by an O–H···O=C hydrogen bond between the carboxy group as donor and the (CF_3)–C=O as acceptor. The hydrogen bond motif is expanded via the 6_5-screw axis into four helices as shown in Fig. 10. Another hydrogen bond exists between N–H and the amide oxygen atom. This hydrogen bond links adjacent helices.

We were also able to obtain and crystallize ketone-derived proline enamines by reacting 1,3-diketones with proline in methanol (Fig. 11).

Remarkably, the structures of the ketone-derived enamines **5a** and **5b** are very similar to the corresponding aldehyde derivatives **3** (see above). Notably, the enamine double bonds in **5a** and **5b** are once again positioned *anti* to the carboxylate (Fig. 12).

Further, the proline conformation for both structures is an envelope, in which the flap is formed by C3 and is in the exo position. The C=C-bond distance is 1.3886(11) Å (**5a**) and 1.3828(8) Å (**5b**). The enamine N–C-bond distance is 1.3358 (10) Å for structure **5a** and 1.3388(7) Å for structure **5b**. The N atoms are only slightly pyramidalized [N pyramidality Δ:

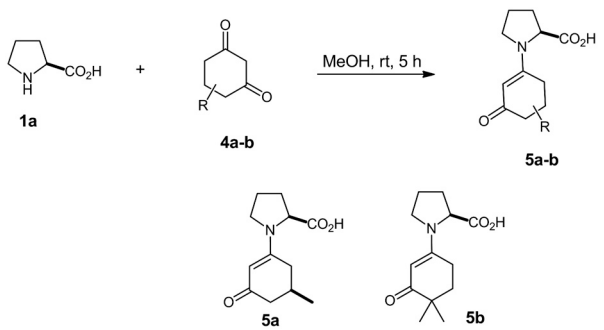

Fig. 11. Synthesis of proline enamines **5a** and **5b**.

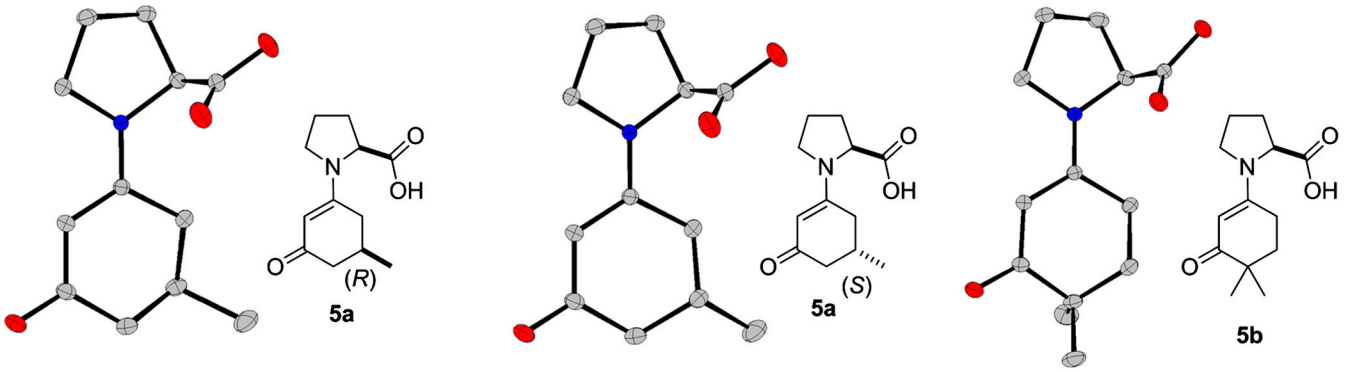

Fig. 12. Crystal structure of enamines **5a** and **5b**. The chiral center in the cyclohexanone ring of **5a** is disordered resulting from crystallization of both diastereomers at the same site.

0.057 Å (**5a**) and 0.017 Å (**5b**)] and the five- and six-membered rings are almost coplanar. Also, as in structures **3**, in both ketone-derived enamines, hydrogen bonds between the carboxylic acid (as donor) and the cyclohexenon carbonyl oxygen atom (as acceptor) are formed. The molecules arrange into chains in a head-to-tail fashion, which are colinear with one of the 2_1-screw axis (parallel to the c axis at ¼ and ½ for **5a** and ¼ and 0 for **5b**) (Fig. 13).

The crystal structures are almost superimposable and only small variations in the dihedral angle of the carboxy group are observed (Fig. 14).

Discussion

Summarizing the above results, several observations have been made: (*i*) Consistent with our hypothesis that resonance interruption should generally favor the enamine constitutional isomer, the corresponding oxazolidinone form is not displayed in any of the 10 structures. Also, potential near attack conformations of a carboxylate oxygen engaging in a reaction with the enamine α-carbon are not observed. Geometric constraints strongly disfavor the required orbital overlap (for C—O distances and a discussion of potential trajectories, *SI Appendix*). Interestingly, this also seems to be true in the anionic carboxylate state: Upon treating enaminone **3d** with triethylamine (1 eq), there is essentially no structural change as confirmed by 1H-NMR spectroscopy (*SI Appendix*). (*ii*) As expected, the studied enamines exclusively display an (*E*)-geometry. (*iii*) Of the 10 structures obtained, 9 display an *anti* arrangement of the carboxylic acid and the enamine double bond. Only in the case of peptide derivative **3g**, which lacks a carboxylic acid attached to the pyrrolidine, is the corresponding *syn* arrangement observed. (*iv*) All enamine structures show intermolecular hydrogen-bonding interactions between the carboxylic acid and the ketone carbonyl group.

It is instructive to compare the obtained crystal structures with the calculated ground and transition state structures (Fig. 15).

As expected, the double bond length (1.382 Å) in the crystal structure of proline enaminone **3a** is longer than that of the calculated enamine ground state of the proline enamine of propionaldehyd (1.341 Å) but quite similar to that in the corresponding transition state (1.385 Å) (12). These structural similarities are also observed in the ketone series: The enamine double bond length in compound **5a** (1.389 Å) and in the cyclohexanone Houk transition state (1.426 Å) are significantly longer than that calculated for the corresponding ground state (1.346 Å) and also that found in a crystal structure of a proline amide-derived cyclohexanone enamine (1.349 Å) previously obtained by Brown et al. (26). Moreover, the enamine C—N bond lengths in the cyclohexanone series are very similar in both the structure of **5a** and the density functional theory structure of the corresponding transition state further validating our transition state/enaminone analogy.

Conclusions

We have described the crystal structures of both aldehyde and ketone-derived proline enaminones and compared their structures with the calculated Houk–List and the postulated Seebach–Eschenmoser transition states. Obviously, one should interpret such structures carefully, and drawing conclusions on possible transition states from crystal structures is challenging in general. Nonetheless, we note that the vast majority of the 10 crystal structures we have been able to obtain are consistent with our previously proposed transition states of proline-catalyzed aldol, Mannich, α-amination, and aminoxylation reactions. After the submission of this manuscript, Schmid et al. have detected aldehyde-derived proline enamines by NMR spectroscopy (27). Remarkably, only the *anti* conformer is observed in solution similarly to the results we report within this manuscript.

ACKNOWLEDGMENTS. We thank Professor K. N. Houk (University of California, Los Angeles) and Professor A. Fu (Qufu Normal University, Shandong,

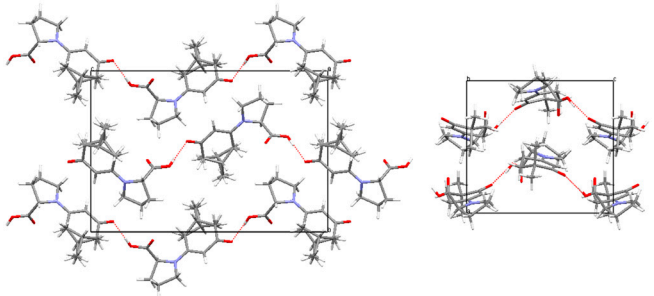

Fig. 13. Crystal packing of enamine **5a** (*Left*) and **5b** (*Right*).

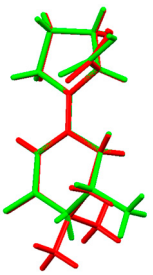

Fig. 14. Superposition of the enamine structures **5a** and **5b**.

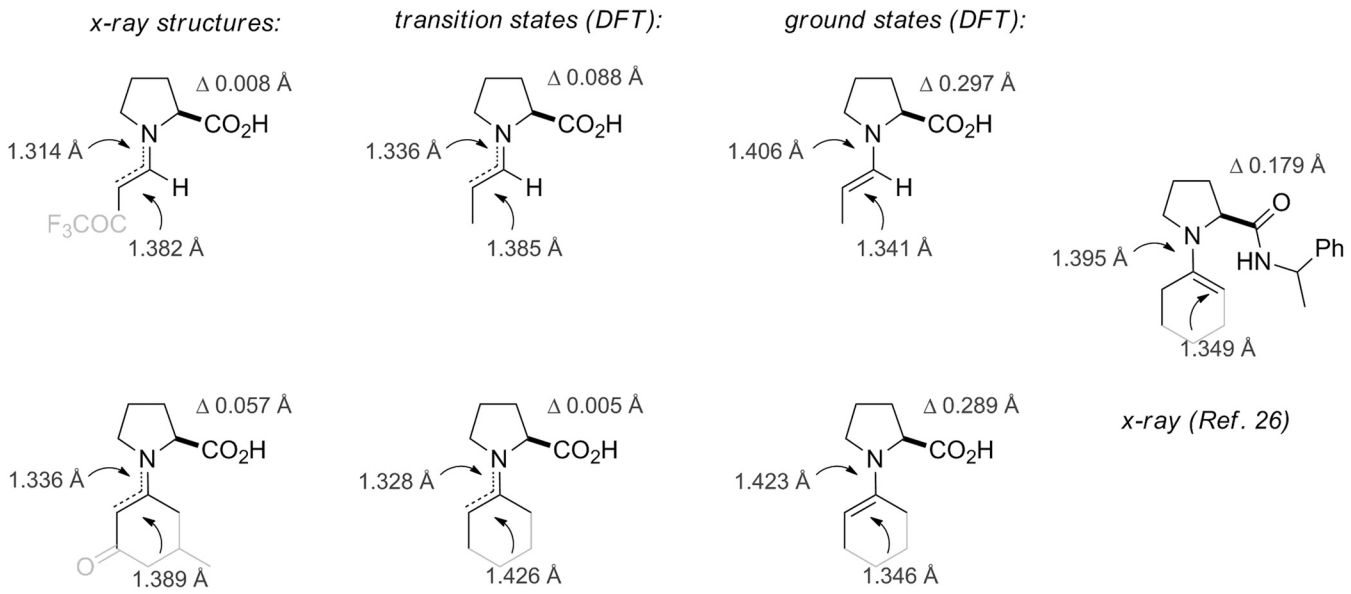

Fig. 15. Comparison of bond lengths and pyramidality of proline enamines.

People's Republic of China) for kindly providing the coordinates of the calculated transition states. Funding was kindly provided by the Max-Planck-Gesellschaft, the Deutsche Forschungsgemeinschaft, and the Fonds der Chemischen Industrie.

1. List B (2005) Enamine catalysis is a powerful strategy for the catalytic generation and use of carbanion equivalents. *Acc Chem Res* 37:548–557.
2. List B (2001) Asymmetric aminocatalysis. *Synlett* 11:1675–1686.
3. List B (2006) The ying and yang of asymmetric aminocatalysis. *Chem Commun* 8:819–824.
4. Mukherjee S, Yang JW, Hoffmann S, List B (2007) Asymmetric enamine catalysis. *Chem Rev* 107:5471–5569.
5. List B (2002) Proline-catalyzed asymmetric reactions. *Tetrahedron* 58:5573–5590.
6. List B, Lerner RA, Barbas CF, III (2000) Proline-catalyzed direct asymmetric aldol reactions. *J Am Chem Soc* 122:2395–2396.
7. Notz W, List B (2000) Catalytic asymmetric synthesis of anti-1,2-diols. *J Am Chem Soc* 122:7386–7387.
8. Bahmanyar S, Houk KN, Martin HJ, List B (2003) Quantum mechanical predictions of the stereoselectivities of proline-catalyzed asymmetric intermolecular aldol reactions. *J Am Chem Soc* 125:2475–2479.
9. Bahmanyar S, Houk KN (2001) Transition states of amine-catalyzed aldol reactions involving enamine intermediates: Theoretical studies of mechanism, reactivity and stereoselectivity. *J Am Chem Soc* 123:11273–11283.
10. Bahmanyar S, Houk KN (2001) The origin of stereoselectivity in proline-catalyzed intramolecular aldol reactions. *J Am Chem Soc* 123:12911–12912.
11. Clemente FR, Houk KN (2004) Computational evidence for the enamine mechanism of intramolecular aldol reactions catalyzed by proline. *Angew Chem Int Edit* 43:5766–5768.
12. Cheong PHY, Houk KN (2004) Origins of selectivities in proline-catalyzed α-aminoxylations. *J Am Chem Soc* 126:13912–13913.
13. Hoang L, Bahmanyar S, Houk KN, List B (2003) Kinetic and stereochemical evidence for the involvement of only one proline molecule in the transition states of proline-catalyzed intra- and intermolecular aldol reactions. *J Am Chem Soc* 125:16–17.
14. List B, Hoang L, Martin HJ (2004) Asymmetric catalysis special feature part II: New mechanistic studies on the proline-catalyzed aldol reaction. *Proc Natl Acad Sci USA* 101:5839–5842.
15. Dane E, Heiss R, Schafer H (1959) Peptid-Synthesen unter Verwendung von Chloral. *Angew Chem* 71:339.
16. Orsini F, et al. (1989) Behaviour of amino acids and aliphatic aldehydes in dipolar aprotic solvents: Formation of oxazolidinones—behaviour of aminoacids and aliphatic aldehydes in dipolar aprotic solvents. *J Heterocyclic Chem* 26:837–841.
17. Seebach D, Boes M, Naef R, Schweizer WB (1983) Alkylation of amino acids without loss of the optical activity: Preparation of α-substituted proline derivatives. A case of self-reproduction of chirality. *J Am Chem Soc* 105:5390–5398.
18. Seebach D, et al. (2007) Are oxazolidinones really unproductive, parasitic species in proline catalysis?—Thoughts and experiments pointing to an alternative view. *Helv Chim Acta* 90:425–471.
19. Marquez C, Metzger JO (2006) ESI-MS study on the aldol reaction catalyzed by L-proline. *Chem Commun* 1539–1541.
20. Andrew RJ, Mellor JM (2000) Synthesis of trifluoromethylpyrroles and related heterocycles from 4-ethyloxy-1,1,1-trifluorobut-3-ene-2one. *Tetrahedron* 56:7267–7272.
21. Luna LE, Seoane G, Cravero RM (2008) Synthesis and characterization of atropisomers arising from 1,3-cyclohexanediones by intermolecular tandem-Michael/Michael additions. *Eur J Org Chem* 7:1271–1277.
22. Friary RJ, Gilligan JM, Szajewski RP, Falci KJ, Franck RW (1973) Heterocyclic synthesis via the intramolecular acylation of enamines derived from amino acids. *J Org Chem* 38:3487–3491.
23. Shreshta-Dawadi PB, Bittner S, Fridkin M, Rahimipour S (1996) On the synthesis of naphthoquinonyl heterocyclic amino acids. *Synthesis* 12:1468–1472.
24. Hajos ZG, Parrish DR (1974) Asymmetric synthesis of bicyclic intermediates of natural product chemistry. *J Org Chem* 39:1615–1621.
25. Gorbunova MG, Gerus II, Galushko SV, Kukhar VP (1991) 4-ethoxy-1,1,1-trifluoro-3-buten-2-one as a new protecting reagent in peptide synthesis. *Synthesis* 3:207–209.
26. Brown KL, et al. (1978) Structural studies of crystalline enamines. *Helv Chim Acta* 61:3108–3135.
27. Schmid MB, Zeitler K, Gschwind RM (2010) The elusive enamine intermediate in proline-catalyzed aldol reactions: NMR detection, formation pathway, and stabilization trends. *Angew Chem Int Edit* 49:4997–5003.